The $R_2Pd_3Ge_5$ (R = La–Nd, Sm) germanides: synthesis, crystal structure and symmetry reduction[&]

Pavlo Solokha[1], Riccardo Freccero[1], Serena De Negri[1], Davide M. Proserpio[2, 3], Adriana Saccone[1]*

[1] Università degli Studi di Genova, Dipartimento di Chimica e Chimica Industriale,
Via Dodecaneso 31, I-16146 Genova, Italy

[2] Università degli Studi di Milano, Dipartimento di Chimica,
Via Golgi 19, 20133 Milano, Italy

[3] Samara Center for Theoretical Materials Science (SCTMS), Samara State University,
Ac. Pavlov Str. 1 Samara 443011, Russia

ABSTRACT

Direct synthesis and structural characterization of a series of new polar rare earth-palladium-germanides of $R_2Pd_3Ge_5$ composition (R = La–Nd, Sm) is reported. The crystal structure of the Nd representative was determined by single crystal X-ray diffraction analysis ($U_2Co_3Si_5$ - type, SG: *Ibam, oI40, Z*=4, *a*=10.1410(6), *b*=12.0542(8), *c*= 6.1318(4) Å, wR2 = 0.0306, 669 F^2 values, 31 variables). The crystal structures of the other homologues were ensured by powder X-ray diffraction pattern analysis. A smooth variation of the cell dimensions is observed through the rare earth series.

The structure of the studied compounds can be interpreted as consisting of a complex three-dimensional $[Pd_3Ge_5]^{\delta-}$ network spaced by the rare earth cations. Within the concept of symmetry reduction, a Bärnighausen tree is used to rationalize the related crystal structures of the RPd_2Ge_2, $RPdGe_3$ and $R_2Pd_3Ge_5$ ternary compounds, enriching the large family of the $BaAl_4$ derivatives.

Moreover, syntheses with metal fluxes were performed, some of which were successful to obtain large crystals of $La_2Pd_3Ge_5$ (using Bi as solvent) and $Nd_2Pd_3Ge_5$ (using Pb as solvent) stoichiometry.

KEYWORDS. Polar intermetallics, Germanides, Crystal structure, Single-crystal X-ray diffraction.

[&] Dedicated to the academician V. Ya. Shevchenko on the occasion of his 75th birthday

[*] To whom the correspondence should be addressed. E-mail: pavlo.solokha@unige.it.
Fax: +39-0103536163. Phone: +39-0103536159.

Introduction

Compounds belonging to the R–T–Tt systems (R = rare earth metal; T = 9th or 10th group metal; Tt = tetrel element) have been extensively studied due to both their structural chemistry variety [1, 2, 3, 4] and interesting properties such as hardness, superconductivity, magnetism, heavy fermion behavior, valence fluctuation, etc. [5, 6, 7]. A bibliographic research was conducted on the R-T-Tt known stoichiometries (≥ 40 at. % Tt), whose results are shown on the Gibbs triangle in figure 1 for germanides. Some stoichiometries have numerous representatives, frequently distributed among different crystal structures.

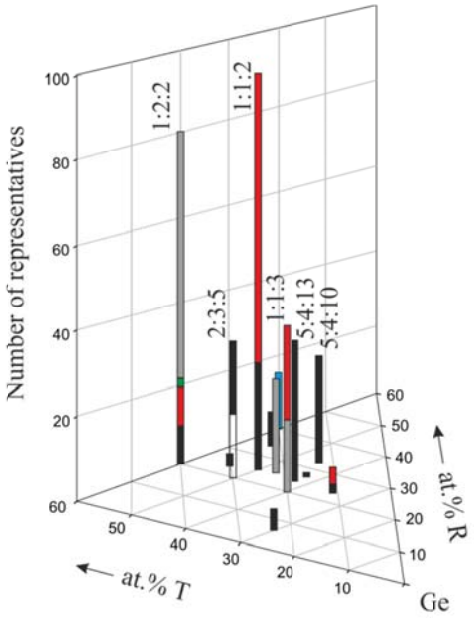

Figure 1. R-M-Ge compounds reported in literature (R = rare earth metal; T= 9th or 10th group metal, content of Ge is bigger than 60 at.%). The most common stoichiometries are indicated. Different colours within the same column correspond to the various crystal structures reported for the same stoichiometry. More details can be found in the Supplementary Material.

The distribution of the two closely related structural modifications (*oI*40 and *mS*40) found for $R_2T_3Ge_5$ compounds is represented in Table 1. The 2:3:5 stoichiometry was observed for all the 9th and 10th group transition elements, in some cases extending along the rare earth series and including ittrium. A structural change from the orthorhombic to the monoclinic form was found for T = Co, Rh on increasing the R atomic number. For the two compounds $\{Pr, Nd\}_2Co_3Ge_5$ both structure-types were detected, the orthorhombic one in samples annealed at 870 K [8, 9], the monoclinic one in samples annealed at 1173 K [2].

Table 1. Structure types of $R_2T_3Ge_5$ compounds (R = rare earth metal; T = 9th or 10th group metal). Data are taken from [1].

R / T	Y	La	Ce	Pr	Nd	Sm	Gd	Tb	Dy	Ho	Er	Tm
Co	■		□	□ ■	□ ■	■	■	■	■	■	■	
Rh	■	□	□	□	■	■	■	■	■	■	■	■
Ir	□	□	□	□	□	□	□	□	□			
Ni			□	□								
Pd						□						
Pt		□		□		□						

□ = *oI*40-$U_2Co_3Si_5$; ■ = *mS*40-$Lu_2Co_3Si_5$

On the other hand, only a few representatives were revealed for the 10th group transition elements; for T = Pd only $Sm_2Pd_3Ge_5$ is known, whose crystal structure was determined by X-ray powder diffraction data [10]. In the framework of our previous investigations on ternary germanides the existence of the $Nd_2Pd_3Ge_5$ compound was established. In this work the results on synthesis and structural characterization of several new $R_2Pd_3Ge_5$ compounds (R = La-Nd, Sm) are reported and discussed. The crystal structure of the title germanides is also presented applying the concept of symmetry reduction as derivative from the RPd_2Ge_2, belonging to the huge family of the derivatives of the ubiquitous $BaAl_4$ aristotype.

The influence of the metal flux on the stabilization of different polymorphs of the same compound was already demonstrated for some binary and ternary tetrelides [7, [11]12,]: for this reason explorative syntheses were conducted on selected $R_2Pd_3Ge_5$ by using different metal fluxes, such as In, Bi and Pb and the obtained preliminary results are also reported in this work.

Experimental

Synthesis and SEM/EDXS characterization

Pure elements were used for the synthesis: lanthanum and neodymium (99.9 mass% purity) were supplied by NewMet Koch, Waltham Abbey, England, palladium (99.95 mass% purity) was supplied by Chimet, Arezzo, Italy, and germanium (99.999 mass% purity) was supplied by MaTecK GmbH, Julich, Germany. Different synthetic routes were followed, including direct synthesis in induction, resistance and arc-furnace and flux synthesis.

The compounds $La_2Pd_3Ge_5$ and $Nd_2Pd_3Ge_5$ were detected in two samples (total mass ~0.8 g) of nominal composition $La_{20.0}Pd_{30.0}Ge_{50.0}$ and $Nd_{22.2}Pd_{11.1}Ge_{66.7}$ respectively, both synthesized in a resistance furnace, with the aim to obtain good quality single crystals. The stoichiometric amounts of the pure elements were enclosed in an arc-sealed Ta crucible, which was then closed in an evacuated

quartz phial to prevent oxidation at high temperature, and finally placed in a resistance furnace, where the following thermal cycle was applied: 25°C (10°C/min) → 950°C →350°C (-0.2°C/min) → 25°C (furnace switched off). A continuous rotation, at a speed of 100 rpm, was applied to the phial during the thermal cycle.

Analogue compounds with R = Ce, Pr and Sm were characterized in as-cast samples with nominal composition $R_{20.0}Pd_{30.0}Ge_{50.0}$, prepared by arc (Ce, Pr) or induction (Sm) melting, with the purpose to confirm the crystal structure. The induction melting procedure was preferred for the Sm-containing sample, in order to avoid any evaporation of this element, which is characterized by a quite high vapour pressure. For this sample, the weighed constituent elements were enclosed in an arc-sealed tantalum crucible and induction melted. The melting was performed under a stream of pure argon and it was repeated several times in order to ensure homogeneity. The Ce and Pr containing samples were synthesized by repeated argon arc melting the elements on a water-cooled copper hearth with a tungsten electrode. Weight losses after arc-melting were generally less than 1%.

In order to investigate the influence of metal flux on phase formation, syntheses with metal solvents were also performed. Lanthanum and Neodymium were chosen for this purpose. Hence, the stoichiometric amounts of elements were put in an arc-sealed Ta crucible with a 1:4 molar excess of metal flux (Bi for the La containing sample; In, Pb and Bi for the Nd containing sample). The total mass of each sample was about 4 g. Then the Ta crucible was closed in an evacuated quartz phial and placed in a resistance furnace, applying the following thermal cycle: 25°C (8°C/min) → 1050°C(2 h) →300°C (-8.0°C/min) → 25°C (furnace switched off). A continuous rotation of the quartz phial during the thermal cycle was applied to favour a better dissolution of the constituting elements inside the flux. A vertical cut of the obtained ingots revealed the presence of large shining crystals, visible to the naked eye, randomly distributed within the flux solidified matrix.

All alloys were submitted to metallographic analysis. Some pieces of each sample were embedded in a phenolic resin with conductive carbon filler, in the automatic hot compression mounting press Opal 410 (ATM GmbH, Germany). Smooth alloys surfaces suitable for microscopic examinations were obtained using the automatic grinding and polishing machine Saphir 520 (ATM GmbH, Germany). SiC papers with grain size decreasing from 600 to 1200 mesh were used for grinding, during which water was used as lubricant. Diamond pastes with particle size decreasing from 6 to 1 μm were used for polishing, using petroleum ether as lubricant. Petroleum ether was also employed to clean samples ultrasonically after each polishing step.

Microstructure examination as well as qualitative and quantitative analyses were performed by a scanning electron microscope (SEM) Zeiss Evo 40 (Carl Zeiss SMT Ltd, Cambridge, England)

equipped with a Pentafet Link Energy Dispersive X-ray Spectroscopy (EDXS) system managed by the INCA Energy software (Oxford Instruments, Analytical Ltd., Bucks, U.K).

X-ray diffraction measurements and crystal structure determination

Single crystals of $Nd_2Pd_3Ge_5$ suitable for X-ray diffraction analysis were selected from the mechanically broken samples and glued on glass fibres. A full-sphere dataset was obtained in routine fashion at ambient conditions on a four-circle Bruker Kappa APEXII CCD area-detector diffractometer equipped by the graphite monochromatized Mo $K\alpha$ ($\lambda = 0.071073$Å) radiation, operating in ω-scan mode. Empirical absorption corrections (SADABS) [13] were applied to all data. Selected crystallographic data and structure refinement parameters are listed in Table **XX**. The structure solution will be described and commented in the "Results and discussion" section. The CIF file, containing details of the structure refinement, is available in the Supplementary Material and it has also been deposited with Fachinformationszentrum Karlsruhe, 76344 Eggenstein-Leopoldshafen, Germany (depository number CSD-431328).

X-ray powder diffraction patterns were recorded on all samples by a diffractometer Philips X'Pert MPD (Cu $K\alpha$ radiation, λ=1.5406 Å, graphite crystal monochromator, scintillation detector, step mode of scanning) in order to ensure the crystal structures of the phases of interest. Sample powders of suitable dimensions were placed in the cavity of a monocrystalline silicon flat holder designed in order to minimize background and zero-shift effects. Powder patterns were collected in the 2θ range 10°-100°, with a scanning step of *ca.* 0.015° and a time per step varying from 10 to 20 sec.

Phase identification was performed with the help of the software PowderCell [14] and lattice parameters were refined by a least-squares method implemented in the software LATCON [15]. Selected powder diffraction patterns are shown in the Supplementary Material.

Results and discussion

Samples characterization by SEM/EDXS analysis

Samples synthesized by slow cooling in the resistance furnace are characterized, as usual, by an inhomogeneous microstructure, containing several different phases, concentrated in the form of large crystals. In the La-containing sample the $La_2Pd_3Ge_5$ compound is the major phase, coexisting with $LaPdGe_3$, $LaPd_{2-x}Ge_{2+x}$, PdGe and Ge, the last three phases in small amount. In the Nd-containing sample, whose nominal composition is farther from the 2:3:5 stoichiometry, the $Nd_2Pd_3Ge_5$ compound coexists with Nd_2PdGe_6, which is the principal phase, and with other unknown ternary phases.

Samples prepared by arc- or induction- melting are almost $R_2Pd_3Ge_5$ single phase, with small amounts of R_2PdGe_6 and Ge. Representative microphotographs are shown in the Supplementary Material.

For the synthesis in metal flux, bismuth was initially chosen, considering some literature data on chemically affine compounds [16]. This metal solvent was found to be a reactive metal flux, forming both binary and ternary compounds, such as $LaBi_2$ (La-Pd-Ge sample); $PdBi_2$ and $Nd_{25}Pd_{25}Bi_{50}$ (Nd-Pd-Ge sample). Nevertheless, the compound of interest was only found in the La-sample in form of quite big, irregularly shaped crystals (see figure 2a).

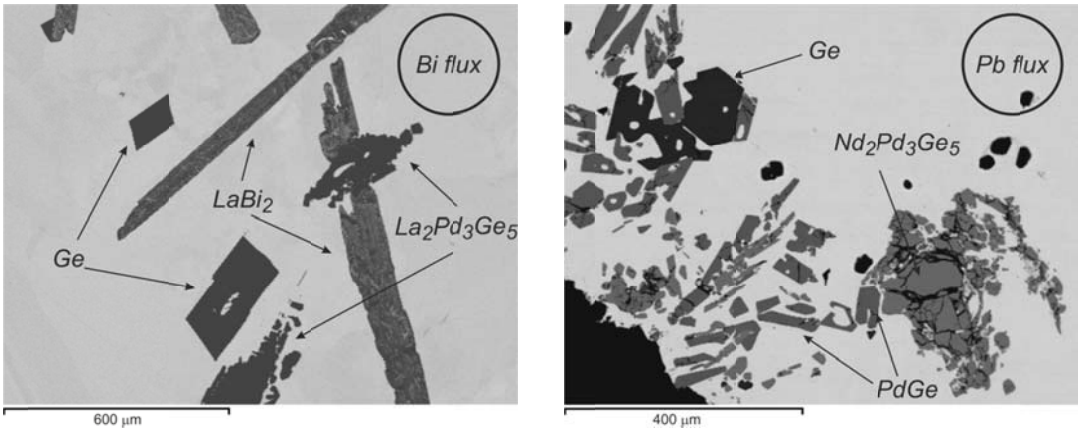

a) b)

Figure 2. Microphographs (BSE mode) of the La-Pd-Ge sample synthesized in Bi-flux (a) and of the Nd-Pd-Ge sample synthesized in Pb-flux (b).

In the Nd-sample the bismuth flux stabilized only the ternary compound $NdPd_2Ge_2$. Therefore, two more metal fluxes (In and Pb) were tested with Nd-Pd-Ge samples. Indium was found to mainly stabilize binary phases such as Pd_3In_7 and $NdGe_2$, with no traces of Nd-Pd-Ge ternary phases. Synthesis in Pb flux was instead successful: big crystals of $Nd_2Pd_3Ge_5$ formed, together with PdGe, re-crystallized Ge (see figure 2b) and other binary and ternary phases not visible in figure 2b. The EDXS measured compositions of the $R_2Pd_3Ge_5$ compounds detected in the studied samples do not noticeably deviate from the ideal stoichiometry (see Table 2).

Table 2. Compositions (measured by EDXS, at.%) and lattice parameters (from X-ray powder spectra) of the $R_2Pd_3Ge_5$ phases detected in the studied samples (* X-ray analysis was not performed).

Rare earth metal	Synthesis method	Composition			Lattice parameters *[Å]*			Volume *[Å^3]*
		R	Pd	Ge	*a*	*b*	*c*	
La	Thermal treatment	20.0	30.1	49.9	10.1834(7)	12.209(1)	6.1898(3)	769.57(7)
La	Bi flux*	19.9	29.3	50.8				
Ce	Arc-melting	20.5	30.6	48.9	10.1511(7)	12.131(1)	6.1568(3)	758.22(7)
Pr	Arc-melting	19.9	31.1	49.0	10.1348(5)	12.0912(8)	6.1363(2)	751.96(6)
Nd	Thermal treatment	19.2	29.7	51.1	10.125(3)	12.036(2)	6.1269(5)	746.7(2)
Nd	Pb flux*	19.3	31.5	49.2				
Sm	Induction melting	19.7	31.3	49.0	10.1160(9)	11.998(1)	6.0911(4)	739.28(9)

Crystal structure of the studied $RE_2Pd_3Ge_5$ compounds

The systematic absences analysis through the recorded data sets were compatible with the orthorhombic *I*-centered space groups *Iba*2 (№ 45) or *Ibam* (№ 75). The preliminary structural model, easily found by *JANA2006* [17], was assumed to contain 1 RE, 2 Pd, and 3 Ge fully occupied sites, taking into account interatomic distances and isotropic displacement parameters. The obtained $RE_2Pd_3Ge_5$ formula is in very good agreement with the EDXS measured compositions. This stoichiometric model was refined, for both single crystals, using full matrix least-squares methods with the *SHELX-14* package programs [18]. The occupancy parameters of all the crystallographic sites were varied in a separate series of least squares cycles along with the displacement parameters but they did not vary noticeably from full occupation and were assumed to be unity in further cycles. No significant residual peaks on differential Fourier maps were detected. This model was then refined anisotropically for both compounds, converging to good residual values. No higher crystallographic symmetry in the tested model was found by *ADDSYM* algorithm implemented in *PLATON* [19].

Details of data collection and refinement are summarized in Table 3. Atomic positions along with isotropic thermal displacement parameters are listed in Table 4. The list of interatomic distances is reported in the Supplementary Material.

Table 3. Crystallographic data for the $Nd_2Pd_3Ge_5$ single crystal and experimental details of the structure determination.

Empirical formula	**$Nd_2Pd_3Ge_5$**
Structure type	$U_2Co_3Si_5$
Crystalline system	Orthorhombic
Space group	*Ibam* (№ 72)
Pearson symbol, Z	*oI*40, 4
EDXS data	$Nd_{20.7}Pd_{31.7}Ge_{47.6}$
Formula weight (M_w, g/mol)	970.63
Unit cell dimensions:	
a [Å]	10.1410(6)
b [Å]	12.0542(8)
c [Å]	6.1318(4)
V [Å^3]	749.6(1)
Calc. density ($D_{calc,}$ g/cm^3)	8.601
Absorption coefficient (μ, mm^{-1})	40.226
Unique reflections	669 (R_{int} =0.0123)
Reflections with I > 2σ(I)	651 (R_{sigma} = 0.0276)
Data/parameters	669/31
Goodness-of-fit on F^2 (S)	1.08
Final R indices [I > 2σ(I)]	R_1 = 0.0136; wR_2 = 0.0303
R indices [all data]	R_1 = 0.0145; wR_2 = 0.0306
$\Delta\rho_{fin}$ (max/min), [e/Å^3]	0.98/-1.03

Table 4. Standardized atomic coordinates and equivalent isotropic displacement parameters (Å^2) for $Nd_2Pd_3Ge_5$.

Atom	*Wyckoff site*	*x/a*	*y/b*	*z/c*	U_{iso}
Nd	8*j*	0.26699(2)	0.37000(2)	0	0.00721(1)
Pd1	8*j*	0.10788(3)	0.13975(2)	0	0.00863(8)
Pd2	4*b*	0.5	0	1/4	0.00904(9)
Ge1	4*a*	0	0	1/4	0.0089(1)
Ge2	8*j*	0.34381(4)	0.10632(4)	0	0.00871(9)
Ge3	8*g*	0	0.27498(3)	1/4	0.00856(9)

The theoretical powder pattern generated from the single crystal model was used to confirm the crystal structure of the analogue 2:3:5 compounds containing La, Ce, Pr and Sm, by using X-ray diffraction powder spectra. As an example, the indexed powder pattern of the almost single phase Ce-Pd-Ge sample is shown in figure 3. Other spectra are available in the Supplementary Material.

The calculated cell volumes are plotted in figure 4 as a function of the radius of the rare earth metal, evidencing a linear decreasing, which reflects the lanthanide contraction. The trivalent radius was considered [20], taking into account literature data on similar 2:3:5 phases [5, 21].

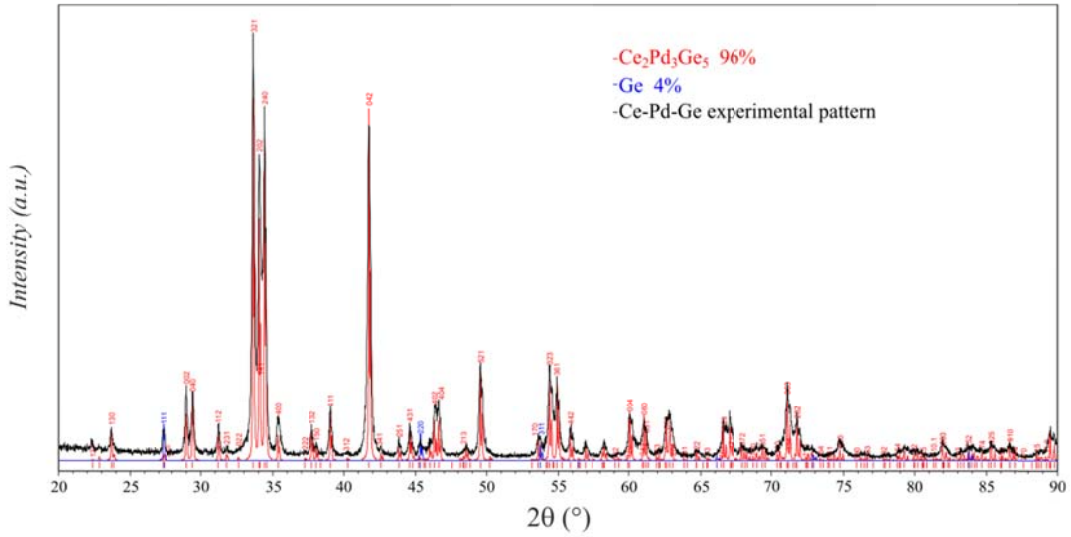

Figure 3. Theoretical (red) and experimental (black) X-ray powder patterns for the Ce-Pd-Ge sample containing the $Ce_2Pd_3Ge_5$ main phase and a small amount of Ge.

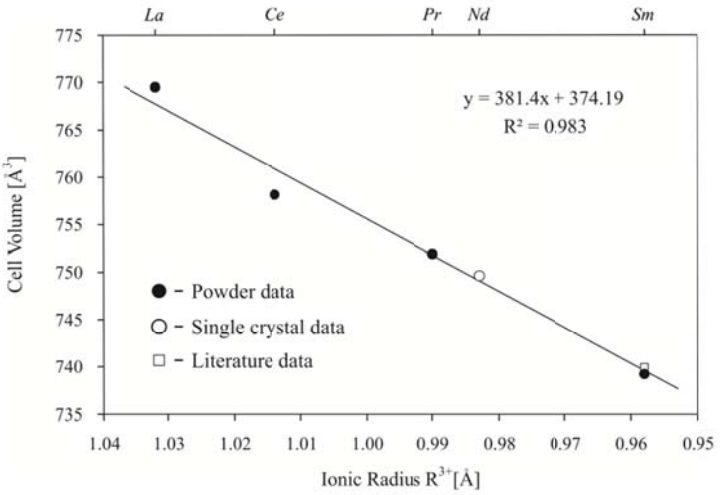

Figure 4. Cell volume of $R_2Pd_3Ge_5$ compounds as a function of the R^{3+} ionic radius (literature data are taken from [10]).

The studied phases crystallize in the orthorhombic *oI*40-$U_2Co_3Si_5$ type, enriching this family with Pd-containing representatives, which were scarcely explored before. The crystal structure of the numerous known $R_2T_3Ge_5$ compounds was studied in detail in the last decades and it was presented from different points of view. According to the geometrical description by Parthé [22, 23], the orthorhombic crystal structure, as well as its monoclinic derivative *mS*40-$Lu_2Co_3Si_5$, could be viewed as an intergrowth of two kinds of structural slabs, related to the $CaBe_2Ge_2$ and to the $BaNiSn_3$ structures respectively. More recently, some authors have interpreted the same structures as consisting of a complex three-dimensional [T_3Ge_5] network spaced by the rare earth cations [11, 24].

Analyzing the connectivity between the species, the latter approach can be reasonably applied also to the $R_2Pd_3Ge_5$ compounds studied here, taking the Nd compound as a representative. The Ge atoms are distributed among three independent crystallographic sites: considering only the Ge-Ge contacts at covalence range distance one can distinguish the presence of isolated Ge atoms (Ge1) and non-planar infinite –(-Ge2-Ge3-Ge2-Ge3-)$_n$– zig-zag chains. Nevertheless, the short Pd-Ge distances, ranging from 2.43 to 2.55 Å (sum of the covalent radii = 2.5 Å [25]), suggest the existence of strong Pd-Ge interactions, being coherent with the idea of a [Pd_3Ge_5] network (see figure 5). In this framework Pd atoms have not homocontacts (d_{min}(Pd-Pd) = 3.07 Å) and are coordinated only by Ge atoms, in two different ways: Pd1 sites are surrounded by five Ge atoms in the form of a distorted square pyramid distanced at about 2.43 (apical position), 2.49 and 2.53 Å (basal positions); Pd2 sites are surrounded by four Ge neighbours at 2.55 Å in the form of a distorted tetrahedron, with two angles being 119.65° and the other two 103.19°. Within this picture, Nd atoms are located in the biggest cavities of the three-dimensional network, being surrounded both by Ge (10 atoms) and by Pd (7 atoms) at distances ranging from 3.06 to 3.49 Å.

Symmetry reduction and crystal structure peculiarities of R-Pd-Ge compounds

Symmetry considerations are more and more applied for comparison of structures, since they allow us to highlight non obvious relationships, for example between structures belonging to different space groups. These relations were definitely formalized within the group theory becoming a part of International Tables (Vol. A1) [26]. In this field, several descriptive works by Bärnighausen and Muller [27, 28, 29], accompanied by real structure examples, clearly showed how to trace out the "symmetry response" of the system with respect to the chemical/physical changes in a very concise and clear manner (the so-called "Bärnighausen tree"). According to this approach, derivative structures are described in term of symmetry reduction with respect to the most symmetrical original structure.

This approach has been used here to rationalize the crystal structure of the R-Pd-Ge ternary compounds containing 20 at.% R, among which the $LaPd_2Ge_2$, $LaPdGe_3$ and $La_2Pd_3Ge_5$ serve as examples. Both $LaPd_2Ge_2$ and $La_2Pd_3Ge_5$ crystal structures could be viewed as derivatives of the $LaPd_2Ge_2$ ($ThCr_2Si_2$-type) structure, which in turn is an ordered ternary derivative of the parent $BaAl_4$-type.

It is worth noting that the "$BaAl_4$ family" of related phases is one of the most populated within the intermetallics. In fact, the multitudinous investigations of the $BaAl_4$-related compounds conducted up to date revealed the existence of an incredible structural variety of them, with numerous representatives in different systems. This study is far away from being complete.

The symmetry reduction principle was recently applied to the $BaAl_4$-type derivatives and a beautiful structural hierarchy tree was constructed [30]. The two branches of this tree concerning the relation between $LaPd_2Ge_2$ ($ThCr_2Si_2$-type) and its 1:1:3 and 2:3:5 derivatives are reproduced in figure 5, together with the corresponding structural distortions/metrical relations of the involved structures.

In all cases the ratio between La and the other two constituent metals is 1 to 4, and the distribution of the rare earth atoms is similar. Instead, the closest arrangement around Pd atoms differs (see figure 5): in $LaPd_2Ge_2$ they are at the centers of $PdGe_4$ distorted tetrahedra (d(Pd-Ge) = 2.51 Å; Ge-Pd-Ge solid angles = 119.8° and 104.6°); in $LaPdGe_3$ palladium atoms are surrounded by five Ge atoms in the form of a square pyramid (d1(Pd-Ge) = 2.46 Å, d2(Pd-Ge) = 2.50 Å), finally, in $La_2Pd_3Ge_5$ an intermediate situation occurs, with two non-equivalent Pd atoms having four and five surrounding Ge, as described above. In fact, the Pd content in the 2:3:5 compound is intermediate between its concentration in 1:2:2 and 1:1:3 stoichiometries.

The symmetry relationships between the considered structures can be highlighted through the Wyckoff positions evolution, which is shown in figure 6.

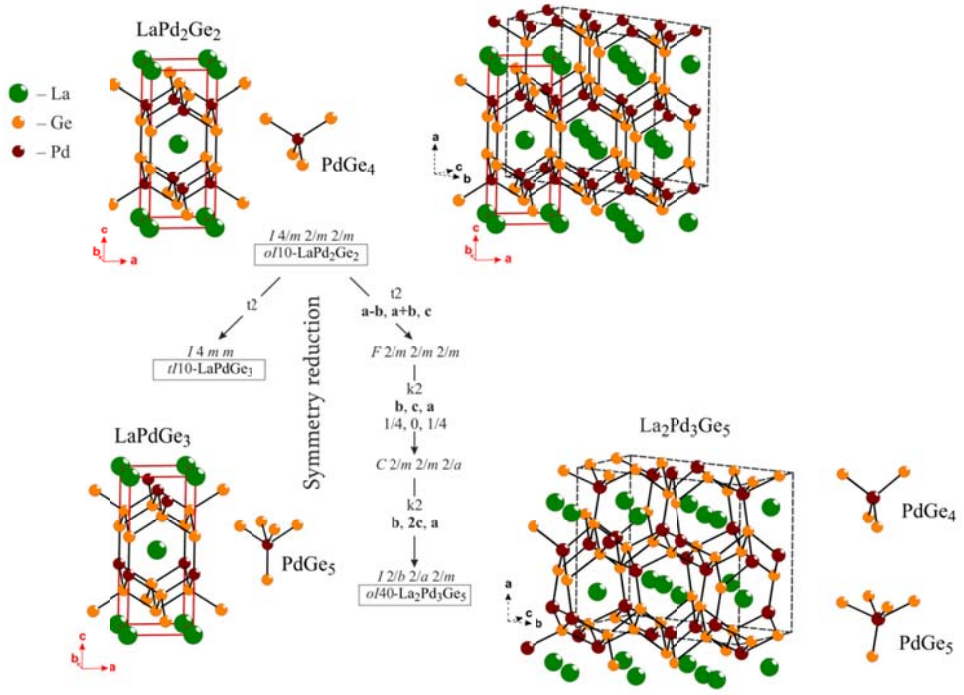

Figure 5. Structural distortion associated with the symmetry reduction from $LaPd_2Ge_2$ to$LaPdGe_3$ (left branch) and to $La_2Pd_3Ge_5$ (right branch). The Pd–Ge 3D networks are indicated by black lines; the closest coordination arrangements for Pd atoms in all structures are evidenced next to each one. The metric relations between structures under consideration are also shown.

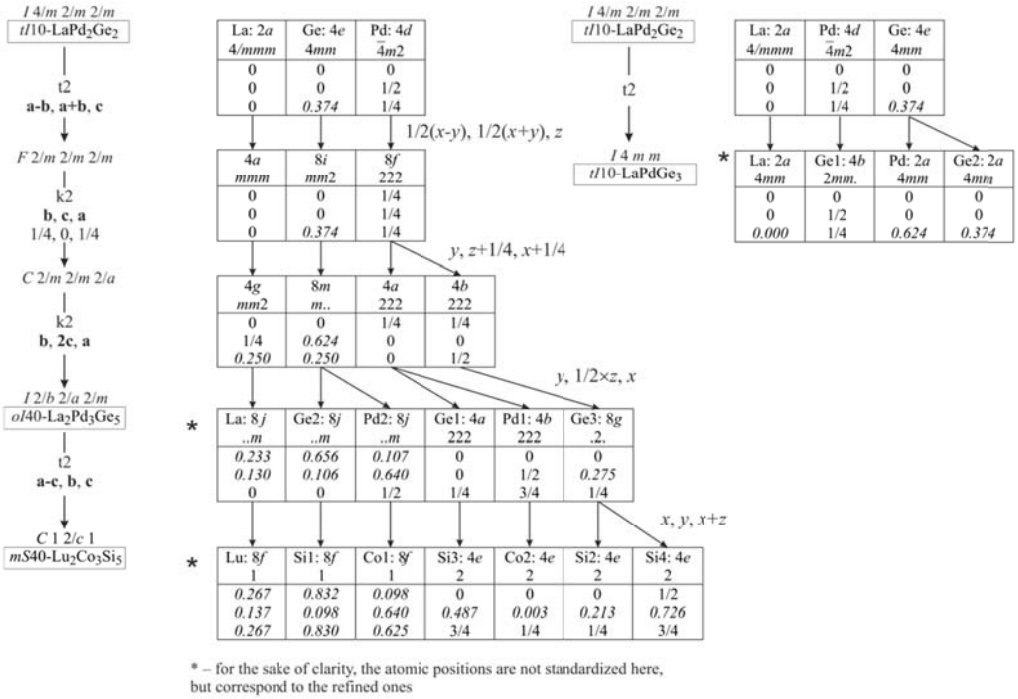

Figure 6. Bärnighausen tree presenting the evolution of the atomic parameters relating the $LaPd_2Ge_2$ with its 2:3:5 and 1:1:3 derivatives.

Analysing this scheme, it becomes clear that, in the derivatives, the rare earth metal suffers a negligible shift with respect to the aristotype and the different stoichiometries originate from different modes of ordered distributions of Pd and Ge species among the split Wyckoff sites. It is worth noting that the Pd and Ge atoms completely occupy their positions, without showing any tendency to statistical mixture.

In agreement with the symmetry principle [28, 29], the shortest way to obtain $LaPdGe_3$ from $LaPd_2Ge_2$ is a one-step *translationengleiche* (t2) decentering, resulting in the splitting of the five coordinated 4*e* site into two 2*a* independent sites. Instead, the orthorhombic $La_2Pd_3Ge_5$ is obtained from the aristotype reducing its symmetry in three steps: a *translationengleiche* (t2) decentering followed by two second order *klassengleiche* transformations (k2), leading to the splitting of both four (4*d*) and five (4*e*) coordinated sites. A further *translationengleiche* (t2) step of symmetry reduction describes the monoclinic $Lu_2Co_3Si_5$ type distorted structure, existing for numerous $R_2T_3Ge_5$ compounds.

The described symmetry reduction steps, mainly concerning the Pd and Ge sites, are responsible for the distortion of the [Pd-Ge] polianionic network, more pronounced for the 2:3:5 structure, also evidenced in figure 5.

Conclusions

The five $R_2Pd_3Ge_5$ compounds (R = La–Nd, Sm) were synthesized and characterized in this work, enriching the $R_2T_3Tt_5$ (R = rare earth metal; T = 9th or 10th group metal; Tt = tetrel element) numerous family with Pd representatives.

Crystal structure determination/confirmation was performed on samples prepared by induction, resistance and arc-furnace melting. The use of molten metals (such as In, Bi, Pb) as solvents for the synthesis of the 2:3:5 compounds was also explored. All the tested fluxes turned out to be reactive, becoming constituents of both binary and ternary compounds. Nevertheless, large crystals of the targeted $La_2Pd_3Ge_5$ and $Nd_2Pd_3Ge_5$ stoichiometries were detected using Bi and Pb solvents respectively. These results are encouraging, since, to our knowledge, only a few ternary germanides were obtained in a similar way up to date. Considering the fact that flux may lead to the stabilization of polymorphs, the structural characterization of the obtained products is necessary and still in progress.

Analyzing the connectivity between the species and literature data on related compounds, the crystal structure of the studied $R_2Pd_3Ge_5$ phases (*oI*40-$U_2Co_3Si_5$ type) was interpreted in terms of a polyanionic Pd-Ge network counterbalanced by rare earth cations. Nonetheless, chemical bonding studies should be carried out in order to confirm this hypothesis and elucidate the role of the transition metal.

Structural relationships among R-Pd-Ge compounds (containing 20 at.% R) were searched for with the help of the group-subgroup theory in the Bärnighausen formalism. The two branches of the symmetry

reduction scheme concerning the relation between the 1:2:2 aristotype and its 1:1:3 and 2:3:5 hettotypes were particularly discussed, highlighting the symmetry principle effectiveness in solid state matter.
Taking into account the outlined peculiarities of Pd and Ge in the studied stoichiometric compounds, the proposed scheme can be used targeting the prediction/modellization of new possible tetrelides, corresponding to different ratios between four- and five- coordinated transition/tetrel elements.

Supplementary Material: X-ray crystallographic file in CIF format, literature data tables and figures, SEM microphotographs, interatomic distances, X-ray diffraction powder patterns, etc. This material is available free of charge via the Internet at ……

REFERENCES

[1] Villars P, Cenzual K (2014/15) Pearson's Crystal Data - Crystal Structure Database for Inorganic Compounds. ASM International, Materials Park, Ohio, USA.

[2] Venturini G, Méot Meyer M, Marêché JF, Malaman B, Roques B (1986) Mat Res Bull 21:33-39.

[3] Venturini G, Malaman B, Roques B (1989) J Less Comm Met 152:51-66

[4] Ohtsu F, Fukuoka H, Yamanaka S (2009) J Alloys Compd 487:712–715

[5] Anand VK, Anupam, Hossain Z, Ramakrishnan S, Thamizhavel A, Adroja DT (2012) J Magn Magn Mat 324 (16): 2483-2487

[6] Kaczorowski D, Pikul AP, Burkhardt U, Schmidt M, Ślebarski A, Szajek A, Werwiński M, Grin Yu (2010) J Phys Condens. Matter 22:215601

[7] Bugaris DE, Sturza M, Han F, Im J, Chung DY, Freeman AJ, Kanatzidis MG (2015) Eur J Inorg Chem:2164–2172

[8] Fedyna MF, Pecharskii VK, Bodak OI (1987) Inorg Mater 23:504-508

[9] Salamakha PS (1997) J Alloys Compd 255:209-220

[10] Barakatova ZM, Seropegin YD, Bodak OI, Belan BD (1995) Russ Metall 1:150-154

[11] Salvador JR, Gour JR, Bilc D, Mahanti SD, Kanatzidis MG (2004) Inorg Chem 43:1403-1410

[12] Tobash PH, Bobev S, Thompson JD, Sarrao JL (2009) J Alloys Compd 488:533–537

[13] Sheldrick GM (1996) SADABS: Siemens Area Detector Absorption Correction Software, University of Goettingen (Germany)

[14] Kraus W, Nolze G (1996) J Appl Crystallogr 29:301-303

[15] Schwarzenbach D (1996) LATCON: Refine Lattice Parameters. Univ Lausanne, Lausanne, Switzerland

[16] Voßwinkel D, Pöttgen R (2013) Z Naturforsch 68b:301-305

[17] Petricek V, Dusek M., Palatinus L (2014) Z Kristallogr 229(5):345-352

[18] Sheldrick GM (2008) Acta Crystallogr A64:112.

[19] Spek AL (2002) PLATON, A Multipurpose Crystallographic Tool. Utrecht University, The Netherlands

[20] Shannon RD (1976) Acta Cryst 32:751

[21] Chevalier B, Lejay P, Etourneau J, Vlasse M, Hagenmuller P (1982) Mat Res Bull 17:1211-1220

[22] Chabot B, Parthè E (1984) J Less-Comm Metals 97:285-290

[23] Chabot B, Parthè E (1985) J Less-Comm Metals 106: 53-59

[24] Zhuravleva MA, Kanatzidis MG (2003) Z Naturforsch 58b:649-657

[25] Emsley J (1999) The Elements, Oxford University Press, Oxford

[26] Wondratschek H, Müller U (2004), International Tables for Crystallography, Vol. A1, Symmetry relations between space groups, Dordrecht, Kluwer Academic Publishers

[27] Bärnighausen H (1980) Commun. Math. Comput. Chem. 9:139-175

[28] Müller U (2013) Symmetry Relationships between Crystal Structures. Applications of Crystallographic Group Theory in Crystal Chemistry. Oxford University Press

[29] Müller U (2006) Inorganic Structural Chemistry (2 ed.). John Wiley&Sons Ltd

[30] Kussmann D, Pöttgen R, Rodewald UCh, Rosenhahn C, Mosel BD, Kotzyba G, Künnen B (1999) Z Naturforsch 54b:1155-1164.